

# Wood Impregnated with a Multicomponent Bio-Phase Change Material for Energy Storage in Buildings

Meysam NAZARI<sup>(a)</sup>, Mohamed JEBRANE<sup>(a)</sup>, Nasko TERZIEV<sup>(a)</sup>

<sup>(a)</sup>Department of Forest Biomaterials and Technology, Swedish University of Agricultural Sciences

Uppsala, Vallvägen 9C, Sweden, [meysam.nazari@slu.se](mailto:meysam.nazari@slu.se)

## ABSTRACT

Wood is widely used in buildings but its low thermal mass limits its energy efficiency for internal use. The thermal mass of wood can be improved by incorporation of PCMs into its porous structure, and thus can control energy intermittency inside buildings. In this study, coconut oil fatty acids mixed with linoleic acid in 4:1 (w/w), with a phase transition temperature in the range of human comfort (18-25 °C), were integrated into thermally treated spruce. The impregnation uptake was 60% and the stability of the PCM in wood structure was evaluated by subjecting impregnated wood samples to leaching tests, and found to be 5%. Thermal characteristics of the wood/BPCM composite including phase transition temperature, enthalpy, heat capacity and thermal conductivity were investigated with DSC, T-history and heat flow meter method, and respectively found to be in the range of 22.4-25.5 °C, 39 J/g, 4 J/(g K) and 0.13 W/(m K).

Keywords: Thermally treated wood, Bio-based PCM, Air conditioning, Energy Efficiency.

## 1. INTRODUCTION

Wood as a renewable material is extensively used in construction due mainly to the high ratio of strength to density (Bal, 2016). The pattern of using wood in building industry has attracted the public attention over the last decade and is expected to grow in the coming years, due to renewability, sustainability and climate benefits (Takano et al., 2014). Spruce timber is one the most used resources of wood-based construction materials in the Nordic countries. Although spruce is a low-permeable (refractory) wood species, it is industrially impregnated with preservatives to prevent the biodegradation in a limited number of applications. An alternative approach to modify spruce timber is thermal modification whereby the wood is heated to temperatures in the range of 180-215 °C for a defined period of time in a medium without oxygen (Esteves and Pereira, 2009). Cellulose and hemicellulose are thermally degraded while lignin is modified to high-molecular structures to reduce the hygroscopicity and improve the dimensional stability of wood.

Although it is extensively used in construction applications, wood's low thermal mass limits its energy efficiency and thermal comfort when used for internal applications (Mathis et al., 2018). One of the pertinent approaches to improve wood's thermal mass is the incorporation of PCMs into its porous structure. PCMs incorporated into wood are considered as effective method to improve the thermal mass and store energy in terms of latent heat. Wood impregnated with PCMs can be used in internal and external joineries to enhance the thermal mass of the building, control temperature fluctuations and improve the thermal comfort in residential buildings (Nazari et al., 2020). Wood engineered with bio-based PCMs, with working temperature between 18-25 °C can absorb extra heat and release it when temperature falls down the comfort temperature providing more comfortable environment inside the building as well as using the energy more efficiently.

## 2. MAIN SECTION

### 2.1. Materials

Thermally treated spruce samples with dimension of 90×90×9 mm were acquired from a local sawmill near Uppsala, Sweden. The thermal treatment (Thermowood®) was carried out at 212 °C. The used bio-based PCM (BPCM) consists of a previously optimized mixture of coconut free fatty acids (CoFA) and linoleic acid (LA) at a proportion of 1:4 (LA/CoFA, w/w). The thermophysical properties of the above BPCM system was already investigated (Nazari et al., 2021).

## 2.2. Methods

### 2.2.1. Impregnation method

BPCM was incorporated into wood samples using a vacuum-pressure process in an autoclave heated at 60 °C. Prior to the BPCM impregnation, wood samples were pre-vacuumed (8 bar for 5 min) to remove the air. The preheated BPCM was introduced into the samples and 5 bar pressure was applied for 30 min, aiming at an uptake of ca. 60%. After conditioning, the impregnated samples were subjected to leaching tests in an oven set at 35 °C for 24 h. The leaching was monitored by measuring samples weight after 2-h intervals, and reported in percentage, the total leakage after 24 h was 5%.

### 2.2.2. Differential Scanning Calorimetry (DSC)

Differential scanning calorimetry (DSC) thermograms were recorded on a Mettler-Toledo DSC 3 system under a nitrogen atmosphere following the same procedure as described in ref (Nazari et al., 2021). Samples of weight in the range of 14-20 mg were taken from the core of each wood/BPCM sample and hermetically sealed in a standard DSC aluminum crucible pan. The DSC tests were conducted between 50 °C and -25 °C at a heating rate of 2 °C/min with 15 min isothermal segment at 50 °C and -25 °C. This heating-cooling cycle was repeated three times to obtain an acceptable reproducibility.

### 2.2.3. T-history method

T-history method was used to measure melting/freezing point, latent heat of fusion, degree of super cooling and specific heat capacity of several samples simultaneously (Nazari et al., 2021). Untreated and treated samples with the BPCM (wood/BPCM composite), and a copper, an aluminum and a stainless steel plates with same dimensions and with known thermal properties were tested simultaneously. The copper plate was used as the main reference to obtain overall heat transfer coefficient ( $U$ ). This parameter was then used to calculate the thermal properties of aluminum and stainless steel, which were then compared with the known data of these materials to verify and validate our approach. The samples and references are thermally insulated using 10 mm thickness ARMAFLEX insulation material. K-type thermocouples were used to record temperature changes over time for samples and references. The thermocouples were placed at the centerline and in the middle of each sample and reference. For cold and hot ambient, two chambers were employed, the former climate chamber was used as cold ambient fixed at 10 °C, while the latter chamber was used as hot ambient fixed at 35 °C. The ambient chamber temperatures were recorded by two thermocouples. Figure 1 shows samples and references with and without insulation. Thermal and physical properties of references are tabulated in table 1.

**Table 1. Thermal and physical properties of the reference metals**

	Copper (SS 5011-04)	Aluminum (SS 4212)	Stainless steel (SS 2343)
Weight (g)	657.6	200.3	581.9
Dimension (mm)	90×90×9	90×90×9	90×90×9
Thermal conductivity (W/(m K))	395	167-216	72-79
Specific heat capacity (J/(g K))	0.385	0.89	0.45-0.46

Samples and references were first preheated at 35 °C, and then quickly transferred into the climate chamber at 10 °C while the temperature profile was recorded. Once the equilibrium temperature was reached (ca. 3 h), the samples and the reference were transferred back at 35 °C and the temperature changes recorded.



**Figure 1: (A) Insulated samples and references inside the chamber. (B) Samples and references without insulation: (a) thermally treated wood/BPCM, (b) thermally treated wood, (c) stainless steel, (d) copper, (e) aluminum.**

Specific heat capacity ( $C_p$ ) of the samples was calculated with the following set of energy balance for reference and samples.

The amount of heat transferred to/from samples inside the oven/chamber is as:

$$Q = UA(T(t)_n - T_\infty) \quad \text{Eq. (1)}$$

where  $Q$ ,  $U$ ,  $A$ ,  $T(t)_n$  and  $T_\infty$  are respectively transferred heat, overall heat transfer coefficient, heat transfer area, sample temperature at each time point and ambient temperature inside oven/chamber.

The amount of heat stored/released from samples is:

$$Q = mC_p \frac{d(T_i - T(t)_n)}{dt} \quad \text{Eq. (2)}$$

where  $m$ ,  $C_p$ ,  $T_i$  and  $dt$  are respectively mass of the samples, specific heat capacity, initial temperature and time interval.

Energy balance inside samples is:

$$Q = -UA(T(t)_n - T_\infty) = mC_p \frac{d(T(t)_n - T_i)}{dt} \quad \text{Eq. (3)}$$

Using energy balance for reference, the term  $UA$  is calculated as follow:

$$\int_{T_i}^{T_n} \frac{d(T(t)_n - T_\infty)}{(T(t)_n - T_\infty)} = - \int_0^{t_n} \frac{UA}{mC_p} dt \quad \text{Eq. (4)}$$

After mathematical operation:

$$\ln \left[ \frac{(T(t)_n - T_\infty)}{(T_i - T(t)_n)} \right] = - \frac{UA}{mC_p} t_n \quad \text{Eq. (5)}$$

Then

$$UA = - \frac{\ln \left[ \frac{(T(t)_n - T_\infty)}{(T_i - T(t)_n)} \right]_{ref}}{t_n} m_{ref} C_{p,ref} \quad \text{Eq. (6)}$$

$UA$  is calculated as above and as heat transfer conditions around reference and samples are the same, then  $UA$  is used for the energy balance of the samples and then  $C_p$  of the samples is calculated as:

$$C_{p,samp} = \frac{\ln\left[\frac{(T(t)_n - T_{\infty})}{(T_i - T(t)_n)}\right]_{ref}}{\ln\left[\frac{(T(t)_n - T_{\infty})}{(T_i - T(t)_n)}\right]_{samp}} \frac{m_{ref}}{m_{samp}} C_{p,ref} \quad \text{Eq. (7)}$$

Enthalpy of the samples is obtained as (Nazari et al., 2021):

$$\Delta H = c_{p,samp}(T(t)_{n,samp} - T_{samp,i}) \quad \text{Eq. (8)}$$

where  $\Delta H$  is the enthalpy.

#### 2.2.4. Thermal conductivity

Thermal conductivity of the composite was measured according to the standard methods ASTM C1155-95 (2013) and ISO 9869-1:2014, known as heat flow meter method with some modifications (Soares et al., 2019). The set up consist of a heat flux sensor and temperature sensors with a specifically designed box. The heat flux sensor integrated with a thermocouple was attached to the sample's surface exposed to the cold environment while the other thermocouple was attached to the sample's surface exposed to the hot environment (Figure 2). Since the purpose was to measure thermal conductivity along the sample's thickness, a well-insulated box was designed to minimize the heat loss from the other sides of the sample. A low heat loss from other sample's directions was assumed as the other dimensions of the samples were ten times larger than the thickness. Two thermocouples K-type and T-type were used to measure the surface temperature on the both sides of the sample. The non-contact surface of thermocouples was insulated to avoid the effect of the ambient temperatures. A heat flux meter, type FHF03 supplied from Hukseflux, the Netherlands was used to measure the heat flux at cold side. The test was run for three hours to ensure a steady state process (Younsi et al., 2008). After measuring the temperatures at both sides and heat flux, the thermal conductivity was calculated according to the Fourier's law as follows:

$$\lambda = \frac{q}{A} \cdot \frac{\Delta L}{\Delta T} \quad \text{Eq. (9)}$$

where  $\frac{q}{A}$  is heat flux,  $\Delta L$  is the thickness, and  $\Delta T$  is temperature difference.

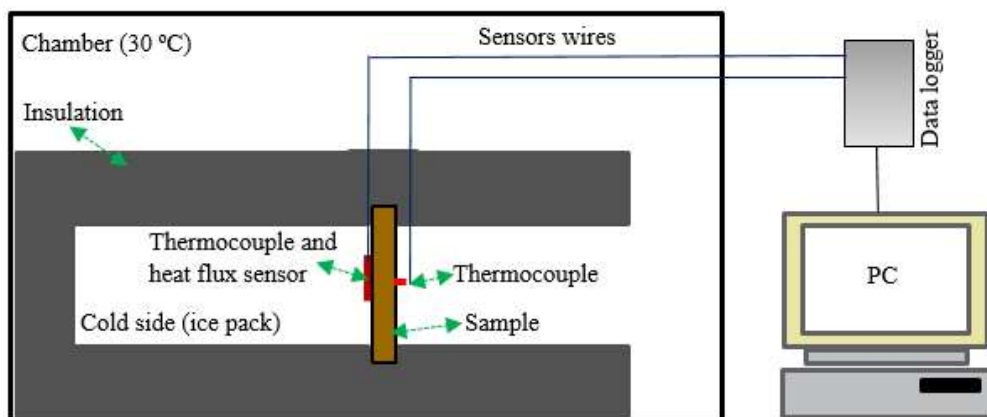
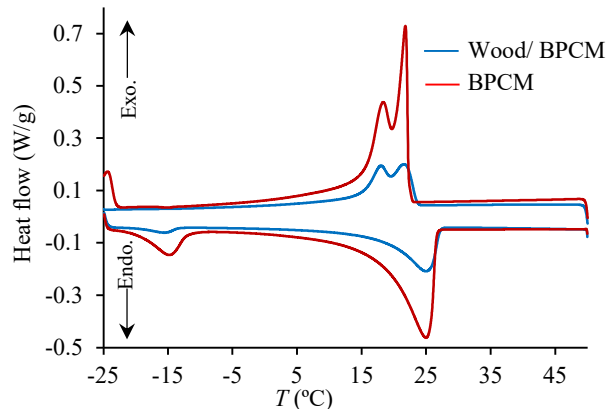


Figure 2: Schematic diagram of the designed rig for thermal conductivity.

### 2.3. Results and discussion

#### 2.3.1. DSC and T-history

Figure 3 shows the DSC curves obtained for the BPCM (Nazari et al., 2021), and thermally treated spruce impregnated with the BPCM. Apparently, the patterns for BPCM and Wood/BPCM composite are similar with small differences in the onset and endset temperatures. The heat flow and enthalpy measured for the wood/BPCM were lower than those recorded for the pure BPCM, as the proportion of BPCM in the composite was approximately 56% and the wood itself does not have latent heat. In addition, the most prominent peak of the pure BPCM decreased after incorporation in wood and two small peaks at lower temperatures, which are probably related to crystalline points of the BPCM were probably shifted to lower temperatures after impregnation into wood. The measured latent heat of fusion for the BPCM was 94 J/g but it was reduced to 39 J/g after incorporation into wood. The thermophysical properties of the BPCM and the composite are tabulated in Table 2.



**Figure 3: DSC thermograms obtained for BPCM ( $x_{LA}=0.2$ ) (Nazari et al., 2021) and Wood/BPCM.**

Figure 4 shows the T-history curves recorded during cooling (a) and heating (b) processes. Compared with DSC, T-history method uses larger sample size without special preparation and thus, the obtained results are more reliable and relevant. The recorded curves showed that wood has less thermal mass compared to stainless steel, copper and aluminum. However, when impregnated with the BPCM, the thermal mass of the composite increased substantially and performing almost as aluminum. During the phase transition, the thermal mass of the composite was comparable to those of stainless steel and copper since it absorbs/releases a reasonable amount of energy during the phase transition. In addition, the BPCM undergoes certain incongruency and supercooling while the BPCM integrated within the composite melts quite congruently and solidifies with no supercooling.

Figure 5a depicts specific heat capacity of wood, wood/BPCM composite, aluminum and stainless steel. In this study, copper was used as a reference material to calculate the overall heat transfer around the samples and subsequently the specific heat capacity of other samples. Aluminum and stainless steel plates were used to verify and validate the results. The measurements showed that the specific heat capacity of aluminum and stainless steel were respectively 0.9 and 0.46 J/(g K) which is in line with the conventional properties of these materials (see Table 1). Previous studies (Simpson and TenWolde, 1999) showed that the heat capacity of wood is temperature and moisture content dependent, and the density and wood species does not influence this property. Early studies showed that the heat capacity of untreated and thermally modified beech were in the range of 1.5-2 J/(g K) at room temperature and 12% moisture content (Simpson and TenWolde, 1999). In this study, the measured heat capacity of the tested samples were in the range of 2-3 J/(g K), which was higher than the reported results in the literature (Simpson and TenWolde, 1999). Few studies investigated thermal properties of thermally modified wood and more studies are needed to investigate the thermal properties of thermally treated wood to gain more reliable results. In addition, Figure 5a reveals that the specific heat capacity of wood/BPCM composite experiences considerable improvement compared to wood. As the specific heat capacity of BPCM was around 5 J/(g K) (Nazari et al., 2021), i.e. higher than that of wood, the specific heat capacity of the composite (wood/BPCM) was in the range of 3-4 J/(g K).

Figure 5b shows the enthalpy of wood and wood/BPCM composite during cooling and heating processes. The wood absorbs and stores only heat in terms of sensible heat, while the composite absorbs and stores both sensible and latent heat. The latent heat of pure BPCM is around 100 J/g (Nazari et al., 2021) but, once incorporated into wood (56% uptake), this value dropped down to around 40 J/g. The overall measured thermal properties by DSC and T-history method of the studied materials are summarized in Table 2. Both methods gave comparable results. The enthalpy of wood/BPCM composite depends on the amount of the impregnated BPCM and its enthalpy but not on the wood itself (Ma et al., 2019).

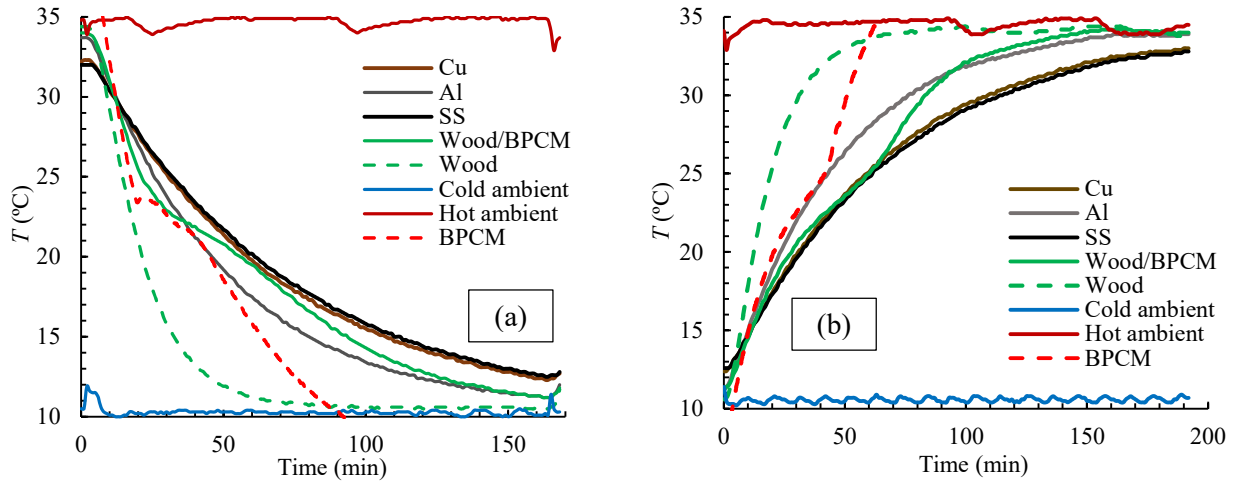


Figure 4: Temperatures vs time from T-history method: (a) Cooling, (b) Heating.

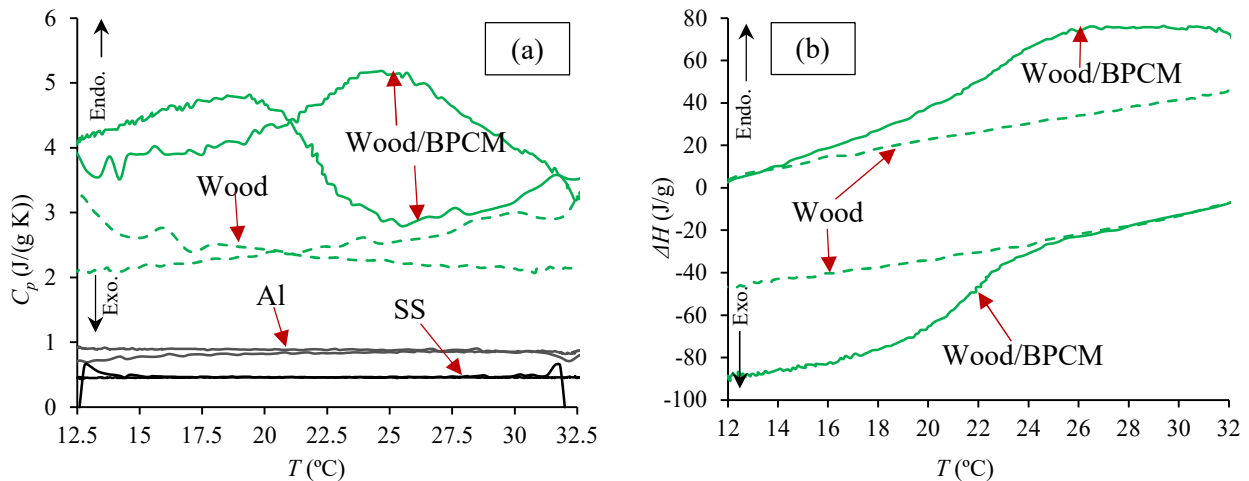
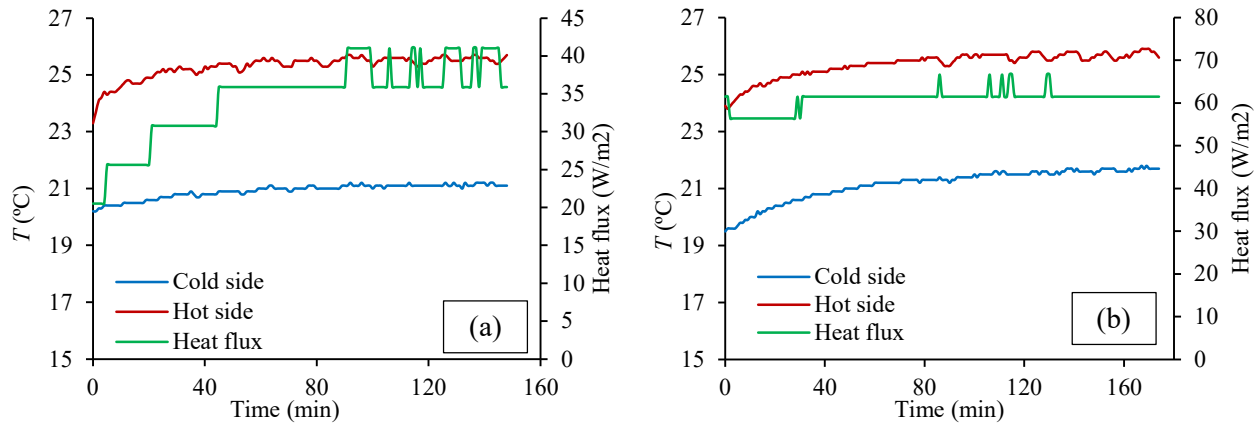


Figure 5: Melting and freezing behaviour of wood and wood/BPCM: (a) specific heat capacity, (b) enthalpy.

### 2.3.2. Thermal conductivity

Figure 6 shows the result from the designed experimental rig of the heat flow meter method. It depicts the temperature and heat flux profiles recorded on both surfaces of the sample. A typical plot of temperature history of wood and wood/BPCM composite is shown in Figure 6a. The tests were performed for ca. 3 h and the temperatures profile reached the steady state after ca. 50 min (Younsi et al., 2008). The obtained results at the steady part of the temperature profiles were used to calculate the thermal conductivity of the samples. The measured thermal conductivity for wood and wood/BPCM composite were respectively 0.08 and 0.13 W/(m K). At liquid state, the thermal conductivity of the BPCM is 0.2 W/(m K) (Nazari et al., 2021), which is higher than that of wood. Incorporation of the BPCM into wood resulted in improvement in thermal conductivity of the composite. The literature data showed that the thermal conductivity varies between wood species and depends upon density and moisture content (Simpson and TenWolde, 1999). The thermal conductivity of spruce was reported to be in the range of 0.11-0.12 W/(m K) at 12% moisture content (Simpson and TenWolde, 1999). In addition, the study reported a reduction in thermal conductivity both in radially and tangentially

directions after thermal modification as a results of lower density and moisture content. This corroborates our results, which are in line with the reported data (Czajkowski et al., 2020). The measured thermal conductivity of the studied materials are summarized in Table 2.



**Figure 6: Measurement of temperatures at both sides and heat flux for thermal conductivity (a) thermally treated spruce, (b) thermally treated spruce impregnated with BPCM.**

**Table 2. Thermal and physical properties of the studied materials, DSC results in parentheses**

	BPCM	Wood	Wood/PCM
Weight (g)	-	30.4	47
Melting point °C	25.5 (24.8)	-	25.5 (26)
Solidifying point °C	21.7 ; 23.7 (18.5; 22)	-	22.4 (15.6; 21.9)
Melting enthalpy J/g	104 (93)	-	38 (38.4)
Solidifying enthalpy J/g	24 ; 54 (92.8)	-	39 (34)
Specific heat capacity J/(g K)	2 ; 5	2-3	3; 4.5
Thermal conductivity W/(m K)	0.2	0.08	0.13

### 3. CONCLUSIONS

In the present study, thermally treated spruce was impregnated with a BPCM to improve the thermal mass of wood for better thermal comfort indoor. Results showed that the impregnation of BPCM into wood resulted in improvement of the thermal mass of the composite compared to the untreated control samples. Additionally, improvements in the specific heat capacity and thermal conductivity were observed for wood/BPCM composite. The impregnated wood has reasonable latent heat of fusion that can absorb and store energy in the range of the human comfort temperature.

### ACKNOWLEDGEMENTS

The study has been carried out within the framework of Smart Energy Systems Research and Innovation Program (ERA-Net E2B2) in the project “Bio-Based Phase Change Materials Integrated into Lignocellulose Matrix for Energy Store in Buildings (BIO-NRG-STORE)”. The authors thank also the financial support by the Swedish Research Council for Sustainable Development (FORMAS), project number 2017-00686.

### NOMENCLATURE

$A$	Heat transfer area (m <sup>2</sup> )	$q$	Heat (W)
$C_p$	Specific heat capacity (J/(g K))	$ref$	Reference
$H$	Enthalpy (J/g)	$samp$	Sample
$i$	Initial	$T$	Temperature (K)

$L$	Thickness (m)	$t$	Time (s)
$m$	Mass (g)	$U$	Overall heat transfer coefficient (W/(m <sup>2</sup> K))
$n$	Time point	$\infty$	Ambient
$Q$	Transferred and stored energy (W)	$\lambda$	Thermal conductivity (W/(m K))

## REFERENCES

- Bal, B.C., 2016. The effect of span-to-depth ratio on the impact bending strength of poplar LVL. *Constr Build Mater* 112, 355–359.
- Czajkowski, Ł., Olek, W. and Weres, J., 2020. Effects of heat treatment on thermal properties of European beech wood. *European Journal of Wood and Wood Products* 78, 425-431.
- Esteves, B. M., Pereira, H. M., 2009. Wood modification by heat treatment: a review. *BioResources*, 4(1), 370-404.
- Ma, L., Wang, Q. and Li, L., 2019. Delignified wood/capric acid-palmitic acid mixture stable-form phase change material for thermal storage. *Solar Energy Materials and Solar Cells* 194, 215-221.
- Mathis, D., Blanchet, P., Landry, V. and Lagièrre, P., 2018. Impregnation of wood with microencapsulated bio-based phase change materials for high thermal mass engineered wood flooring. *Applied Sciences* 8(12), 2696.
- Nazari, M., Jebrane, M. and Terziev, N., 2020. Bio-Based Phase Change Materials Incorporated in Lignocellulose Matrix for Energy Storage in Buildings-A Review. *Energies*, 13(12), 3065.
- Nazari, M., Jebrane, M. and Terziev, N., 2021. Multicomponent bio-based fatty acids system as phase change material for low temperature energy storage. *Journal of energy storage* 39, 102645.
- Simpson, W., TenWolde, A., 1999. Physical properties and moisture relations of wood. In: *Wood handbook: wood as an engineering material*. Madison, WI: USDA Forest Service, Forest Products Laboratory, 1999. General technical report FPL, 3.1-3.24.
- Soares, N., Martins, C., Gonçalves, M., Santos, P., da Silva, L.S. and Costa, J.J., 2019. Laboratory and in-situ non-destructive methods to evaluate the thermal transmittance and behavior of walls, windows, and construction elements with innovative materials: A review. *Energy and Buildings* 182, 88-110.
- Takano, A., Hughes, M. and Winter, S., 2014. A multidisciplinary approach to sustainable building material selection: A case study in a Finnish context. *Building and Environment* 82, 526-535.
- Younsi, Z., Joulin, A., Zalewski, L., Lassue, S. and Rouse, D., 2008. Thermophysical characterization of phase change materials with heat flux sensors. *Proceedings of Eurotherm, The Netherlands*. ISBN 978-90-386-1274-4.